ISSN 0023-1584, Kinetics and Catalysis, 2009, Vol. 50, No. 2, pp. 275–283. © Pleiades Publishing, Ltd., 2009.
Original Russian Text © I.S. Yakovleva, L.A. Isupova, V.A. Rogov, 2009, published in Kinetika i Kataliz, 2009, Vol. 50, No. 2, pp. 290–299.

Oxygen Species and Their Reactivity in the Mechanochemically Prepared Substituted Perovskites $La_{1-x}Sr_xCoO_{3-y}$ (x = 0–1)

I. S. Yakovleva, L. A. Isupova, and V. A. Rogov

Boreskov Institute of Catalysis, Siberian Branch, Russian Academy of Sciences, Novosibirsk, 630090 Russia
e-mail: irga@catalysis.ru

Received September 21, 2007

Abstract—The oxygen species and their reactivity in the mechanochemically prepared substituted perovskites $La_{1-x}Sr_xCoO_{3-y}$ were studied using temperature-programmed reduction (TPR) of the samples with hydrogen. The experimental data were compared with data on the catalytic activity of the series of $La_{1-x}Sr_xCoO_{3-y}$ catalysts in the oxidation of CO, as well as with the real structures and surface compositions of the samples, which were studied in detail previously. As the strontium content was increased, the degree of reduction of the samples increased in the course of TPR and the TPR peaks shifted to the region of lower temperatures, except for the last sample containing no lanthanum (x = 1). An increase in the calcination temperature and time resulted in a decrease in TPR peak intensities and in a shift of the peaks to the region of higher temperatures. A reaction scheme was proposed for the reduction. In accordance with this reaction scheme, Co^{4+} in substituted cobaltites was reduced to Co^0 at temperatures lower than 400°C. In the temperature region of 400–500°C, the $Co^{3+} \longrightarrow Co^{2+}$ bulk reduction, as well as the deep reduction processes $Co^{3+} \longrightarrow Co^0$ and $Co^{4+} \longrightarrow Co^0$, occurred; substitution facilitated the above processes. At temperatures higher than 500°C, $Co^{2+} \longrightarrow Co^0$ bulk reduction occurred. The observed reduction of the mechanochemically prepared samples depended on their microstructure, which was described previously. It was found that the activity of the samples in the oxidation of CO depends on the amount of the most weakly bound reactive surface oxygen species, which were removed in TPR with hydrogen to 150°C. No correlation between the amount of strongly bound (lattice) oxygen removed upon TPR and the activity of $La_{1-x}Sr_xCoO_{3-y}$ samples in the oxidation of CO was found.

DOI: 10.1134/S0023158409020190

INTRODUCTION

Transition metal oxides and rare earth oxides with a perovskite structure, which are characterized by high thermal stability and resistance to reaction atmospheres under severe conditions, are actively used in various promising high-temperature processes such as the catalytic combustion of hydrocarbons, the steam reforming of methane, the oxidation of ammonia, and the reduction of sulfur dioxide [1–3]. Substituted perovskites, including the series of $La_{1-x}Sr_xCoO_{3-y}$, which exhibit unique physicochemical properties, are of the greatest interest. An analysis of published data suggests that the properties (including catalytic properties) of substituted perovskites depend on the sample preparation conditions.

Isupova et al. [4] performed a systematic study of a series of mechanochemically prepared $La_{1-x}Sr_xCoO_{3-y}$ perovskites. The mechanochemical method, which is a new rapid and almost wasteless synthetic method, allowed us to shorten considerably the sample preparation time (from tens or even hundreds of hours to 3–4 h) and temperature (from 1100–1200 to 900–1100°C), as compared with the traditional ceramic synthesis method. It was found that the microstructure peculiarities of the mechanochemically prepared samples are the microheterogeneous structure of a near-surface layer of particles and the segregation of elements (the near-surface enrichment of particles in strontium and cobalt cations).

The catalytic properties of the $La_{1-x}Sr_xCoO_{3-y}$ system were studied in the model reaction of CO oxidation, and a nonmonotonic change in the specific catalytic activity upon the replacement of lanthanum by strontium was found [4]. In the series of samples calcined at 900°C, a sample with x = 0.3 exhibited the highest activity. In the samples calcined at 1100°C, two catalytic activity maximums were observed in samples with x = 0.3 and 0.8. It was found that the catalytic activity maximums of these samples correlated with the formation of microheterogeneity in these samples; it is likely that this microheterogeneity was responsible for the presence of weakly bound oxygen.

The conclusion that catalytic activity is due to the presence of weakly bound oxygen in microheterogeneous samples from the series of $La_{1-x}Sr_xCoO_{3-y}$ is qualitative, and information on the particular active oxygen species responsible for the activity of this series in redox reactions is required. Therefore, in this work, we studied oxygen species and their reactivity charac-

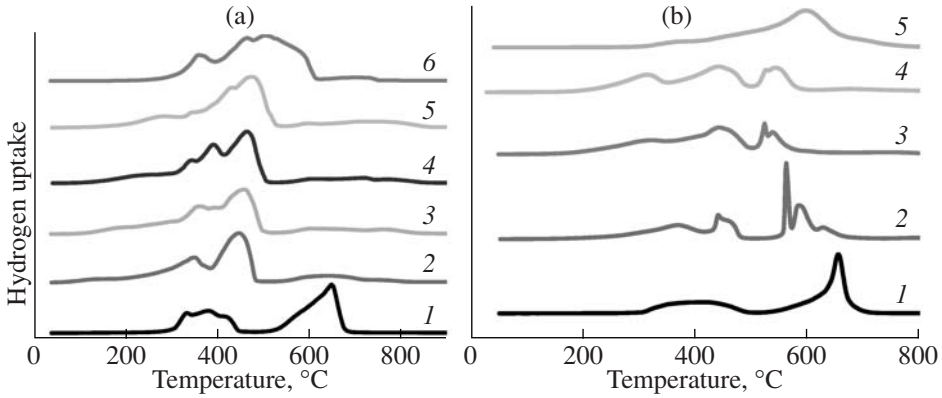

Fig. 1. TPR curves for perovskites from the series of $La_{1-x}Sr_xCoO_{3-y}$: (a) T_{calcin} = 900°C; x = (*1*) 0, (*2*) 0.3, (*3*) 0.4, (*4*) 0.6, (*5*) 0.8, and (*6*) 1; (b) T_{calcin} = 1100°C; x = (*1*) 0, (*2*) 0.3, (*3*) 0.6, (*4*) 0.7, and (*5*) 1.

teristics using the temperature-programmed reduction (TPR) of $La_{1-x}Sr_xCoO_{3-y}$ samples with hydrogen.

EXPERIMENTAL

La_2O_3, $SrCO_3$, and Co_3O_4 (reagent grade) were used as the starting compounds for the synthesis.

The mechanochemical synthesis of $La_{1-x}Sr_xCoO_{3-y}$ samples (x = 0, 0.2, 0.4, 0.6, 0.8, and 1) was performed by the calcination of mechanically preactivated mixtures of the starting oxides taken in appropriate ratios at 900 or 1100°C for 4 h. The mechanochemical treatment time was 3 min; the procedure of this synthesis was described previously [4].

The catalytic activity in the oxidation of CO was determined at 190–230°C in a flow-circulation reactor with chromatographic analysis for a catalyst fraction of 0.5–1 mm. The catalytic experiments were described in detail elsewhere [4].

The TPR of the samples with hydrogen was studied in a flow system with a thermal-conductivity detector for a size fraction of 0.25–0.5 mm. Before the reduction, the samples were trained in O_2 at 500°C for 0.5 h and cooled to room temperature in O_2. The sample weight was 50 mg; the flow rate of the reducing mixture (10% H_2 in Ar) was 40 cm^3/min. The samples were heated to 900°C at a rate of 10 K/min. The amount of absorbed hydrogen (mmol/g_{sample}) was determined from areas under the TPR curves of the samples; the integration was performed using the Origin 6.0 program.

The number of oxygen monolayers removed at low TPR temperatures was estimated from the relationship

$$N_{\text{monolayers O}_2} = (6 \times 10^{23} \int \text{H}_2)/(1.09 \times 10^{19} S_{\text{sp}} m),$$

where $\int \text{H}_2$ is the absorption of hydrogen in the region of low TPR temperatures, mol; 6×10^{23} is the Avogadro number, mol^{-1}; 1.09×10^{19} is the number of sites in a monolayer per surface square meter, m^{-2}; S_{sp} is the specific surface area, m^2/g; and m is the sample weight, g.

RESULTS AND DISCUSSION

TPR of $La_{1-x}Sr_xCoO_{3-y}$ Samples with Hydrogen

Figure 1 shows TPR curves (the dependences of the absorption of hydrogen on sample reduction temperature) for various degrees of substitution (x) and preparation conditions (calcination temperature and time). The complicated shape of the TPR curves of the $La_{1-x}Sr_xCoO_{3-y}$ samples suggests that the reduction of the samples with hydrogen occurred in various temperature regions. This can be due to both various surface and lattice oxygen species in perovskites and the complex microstructure of the samples [4]. We distinguished the following three main regions of hydrogen consumption:

(1) low-temperature consumption, which quantitatively corresponds to the removal of no more than a monolayer surface coverage with oxygen (to 150°C);

(2) consumption with maximums in the temperature region below 500°C, which corresponds quantitatively to the reduction of Co^{4+} and Co^{3+} cations to Co^{2+} and Co^0;

(3) consumption in the temperature region above 500°C, which corresponds quantitatively to the bulk reduction $Co^{2+} \longrightarrow Co^0$ with the degradation of perovskite.

Tables 1 and 2 summarize the data concerning the hydrogen uptake in each particular region and the total uptake. These data suggest that the reducibility of LaSrCo perovskites increased with the degree of substitution (x); however, this dependence was intricate. Thus, an increase in the strontium content caused a nonmonotonic change in the hydrogen uptake in the first (to 150°C) and second (to 500°C) temperature regions (Tables 1 and 2, respectively; Fig. 2). At the same time, the total amount of hydrogen consumed in the course of TPR increased with the strontium content (Fig. 2). The

Table 1. Hydrogen uptake by $La_{1-x}Sr_xCoO_{3-y}$ samples calcined at 1100°C in the course of TPR in various temperature regions

Sample composition x	Hydrogen uptake, mol/g			
	40–150°C, region 1, $\times 10^5$	150–500°C, region 2, $\times 10^3$	500–900°C, region 3, $\times 10^3$	40–900°C, total uptake, $\times 10^3$
0	2.56	2.16	3.75	5.94
0.3	4.54	3.43	3.12	6.60
0.6	3.56	5.39	2.02	7.45
0.7	2.37	5.46	2.57	8.05
1.0	1.78	2.08	6.29	8.39

Table 2. Hydrogen uptake by $La_{1-x}Sr_xCoO_{3-y}$ samples calcined at 900°C in the course of TPR in various temperature regions

Sample composition x	Hydrogen uptake, mol/g			
	40–150°C, region 1, $\times 10^5$	150–500°C, region 2, $\times 10^3$	500–900°C, region 3, $\times 10^3$	40–900°C, total uptake, $\times 10^3$
0	2.86	2.43	3.66	6.12
0.3	17.4	5.34	1.04	6.55
0.4	13.1	5.88	1.15	7.16
0.6	8.79	6.33	1.07	7.49
0.8	2.35	6.30	1.42	7.74
1.0	1.29	5.21	3.85	9.07

results of data processing also indicate that the hydrogen uptake depended on not only the composition of the samples but also the calcination temperature: the peaks of reduction shifted to the region of higher temperatures as the calcination temperature was increased.

Based on the total uptake, the oxygen nonstoichiometry y was calculated for each sample from the $La_{1-x}Sr_xCoO_{3-y}$ series (Table 3), and the concentrations of Co^{4+} and Co^{3+} cations were calculated from electrical neutrality (Table 3). Figure 3a shows the dependence of the oxygen nonstoichiometry y on the composition x and calcination temperature. It can be seen that an increase in the calcination temperature caused a decrease in the oxygen content, whereas the dependence of y on the strontium content changed in an intricate manner with a maximum for the sample with $x = 0.4$. Figure 3b shows the dependence of the concentration of Co^{4+} cations on the composition and calcination temperature. It is natural that the concentration of Co^{4+} cations was higher in the samples calcined at 900°C as compared with those calcined at 1100°C. The dependence of the concentration of Co^{4+} on the strontium

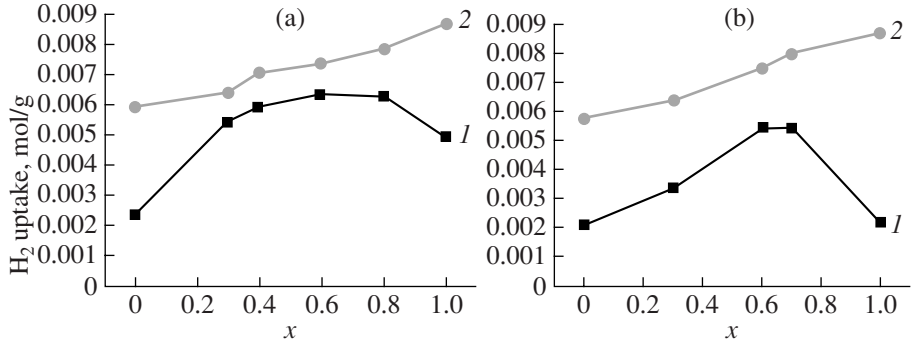

Fig. 2. Dependence of the amount of consumed hydrogen on the sample composition (x) in TPR temperature regions (*1*) up to 500 and (*2*) up to 900°C for $La_{1-x}Sr_xCoO_{3-y}$ calcined at (a) 900 and (b) 1100°C.

Table 3. Stoichiometric composition of $La_{1-x}Sr_xCoO_{3-y}$ samples calcined at 900 and 1100°C calculated from the total uptake of oxygen

x	T = 900°C	T = 1100°C
0	$La(Co_{0.97})^{3+}(Co_{0.03})^{4+}O_{3.015}$	$LaCoO_3^*$
0.3	$La_{0.71}Sr_{0.31}(Co_{0.37})^{4+}(Co_{0.63})^{3+}O_{3.06}$	$La_{0.7}Sr_{0.3}(Co_{0.25})^{4+}(Co_{0.75})^{3+}O_{2.95}$
0.4	$La_{0.66}Sr_{0.34}(Co_{0.44})^{4+}(Co_{0.56})^{3+}O_{3.11}$	–
0.6	$La_{0.4}Sr_{0.6}(Co_{0.40})^{4+}(Co_{0.60})^{3+}O_{2.90}$	$La_{0.4}Sr_{0.6}(Co_{0.26})^{4+}(Co_{0.74})^{3+}O_{2.83}$
0.7	–	$La_{0.3}Sr_{0.7}(Co_{0.51})^{4+}(Co_{0.49})^{3+}O_{2.91}$
0.8	$La_{0.2}Sr_{0.8}(Co_{0.64})^{4+}(Co_{0.36})^{3+}O_{2.92}$	–
1.0	$Sr(Co_{0.80})^{4+}(Co_{0.04})^{3+}O_{2.66}$	$Sr(Co_{0.47})^{4+}(Co_{0.42})^{3+}O_{2.57}$

* $La_{0.995}CoO_{2.9925}$.

content changed in an intricate manner: initially, the concentration of Co^{4+} cations increased to reach a local maximum in the sample with $x = 0.4$. In the series of samples calcined at 900°C, this was accompanied by an increase in excessive oxygen (the positive oxygen nonstoichiometry reached a maximum in the sample with $x = 0.4$). Then, the relative fraction of vacancies began to increase, and the fraction of Co^{4+} cations decreased; this is consistent with published data [5]. However, the concentration of Co^{4+} in the series of compositions reached a maximum (as well as the concentration of vacancies) in the sample with $x = 1$.

The above data indicate that the TPR of cobaltites from the series of $La_{1-x}Sr_xCoO_{3-y}$ resulted in the bulk reduction of the samples to form cobalt metal. The TPR data will be considered below in more detail in accordance with the division into three groups (Tables 1, 2); the corresponding reduction processes and detected oxygen species will be compared with catalytic activity.

Reduction of $La_{1-x}Sr_xCoO_{3-y}$

Tables 4 and 5 summarize the models of reduction based on the processing of TPR data and the ratios between Co^{4+} and Co^{3+} cations. In the calculations, we assumed that the bulk reduction $Co^{2+} \longrightarrow Co^0$ occurred in the temperature region above 500°C. Then, we calculated the concentration of Co^{3+} cations, from which Co^{2+} cations were formed (at the first step of reduction in the reaction $Co^{3+} \longrightarrow Co^{2+}$). The remaining amount of hydrogen absorbed in the temperature region below 500°C was attributed to the reduction processes $Co^{4+} \longrightarrow Co^{2+}$, $Co^{3+} \longrightarrow Co^0$, and $Co^{4+} \longrightarrow Co^0$.

As can be seen in reaction schemes in Tables 4 and 5, the cation reduction processes $Co^{4+} \longrightarrow Co^{2+}$, $Co^{3+} \longrightarrow Co^{2+}$, $Co^{4+} \longrightarrow Co^0$, and $Co^{3+} \longrightarrow Co^0$ occurred in the TPR temperature region below 500°C, whereas the bulk reduction $Co^{2+} \longrightarrow Co^0$ occurred above 500°C. The particular reaction scheme of reduction depended on both the sample composition and the sample preparation temperature.

$La_{1-x}Sr_xCoO_{3-y}$ samples at T_{calcin} = 1100°C. The unsubstituted sample of $LaCoO_3$ was reduced in two steps: the cation reduction $Co^{3+} \longrightarrow Co^{2+}$ occurred in the region below 500°C, and the bulk reduction $Co^{2+} \longrightarrow Co^0$ occurred above 500°C. This is consistent with well-known published data. Thus, for example, Futai and Yonghua [8] also observed the reduction of rare earth (including lanthanum) cobaltites in two steps. At the first step, the anion-deficient perovskite

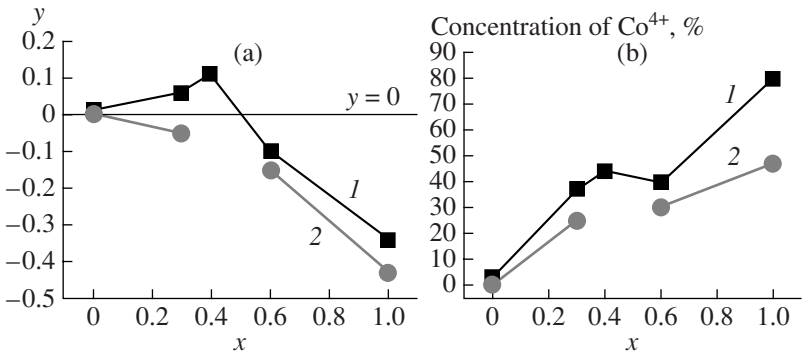

Fig. 3. Dependence of the oxygen nonstoichiometry y and the concentration of Co^{4+} cations on the composition of $La_{1-x}Sr_xCoO_{3-y}$ and calcination temperature: (*1*) 900 and (*2*) 1100°C.

Table 4. Reduction of $La_{1-x}Sr_xCoO_{3-y}$ samples calcined at 1100°C in particular regions of hydrogen uptake

x	Uptake regions (1 + 2) (40–500°C)	Uptake region (3) (500–900°C)	Cationic species ratio Co^{4+}/Co^{3+} (calculated from (1 + 2) and (3))
0	94% $Co^{3+} \longrightarrow Co^{2+}$ (410°C)* 5.4% $Co^{3+} \longrightarrow Co^0$	94% $Co^{2+} \longrightarrow Co^0$ (654°C)	0.006/0.994
0.3	25% $Co^{4+} \longrightarrow Co^0$ (365°C) 61% $Co^{3+} \longrightarrow Co^{2+}$ (440°C)	72% $Co^{2+} \longrightarrow Co^0$ (565°C)	0.25/0.72
0.6**	(1): 24% $Co^{4+} \longrightarrow Co^0$ (316°C) (2): 30% $Co^{3+} \longrightarrow Co^{2+}$ (385°C) (3): 40% $Co^{3+} \longrightarrow Co^0$ (523°C)	(4 + 5 + 7): 35% $Co^{2+} \longrightarrow Co^0$ (523°C) (6): 4% $Co^{3+} \longrightarrow Co^0$ (603°C)	0.24/0.74
0.7**	(1): 18% $Co^{4+} \longrightarrow Co^0$ (307°C) (2): 2% $Co^{3+} \longrightarrow Co^0$ (385°C) (3): 55% $Co^{3+} \longrightarrow Co^{2+}$ and 27% $Co^{4+} \longrightarrow Co^0$ (444°C)	(4 + 5): 55% $Co^{2+} \longrightarrow Co^0$ (541°C)	0.45/0.57
1.0	~40% $Co^{3+} \longrightarrow Co^0$ (~500°C) ~43% $Co^{4+} \longrightarrow Co^0$ (~600°C) The processes occur almost continuously		0.43/0.40

*The corresponding peak temperatures (T_{max}) are given in parentheses.

**Uptake in different temperature regions was calculated with the use of an asymmetric function approximation (Figs. 6a, 6b).

$ReCoO_{2.5}$ (peak T_{max} ~400°C) was formed, whereas cobalt metal Co^0 (peak T_{max} ~ 600°C) was formed at the second step.

An excess absorption in the region of low temperatures suggests the deeper reduction of a portion (5%) of Co^{3+} cations by the reaction $Co^{3+} \longrightarrow Co^0$ (Table 4). In the region of temperatures lower than 130°C, the amount of weakly bound surface oxygen, which is removed in this TPR region, and the number of removed monolayer surface coverages with oxygen were estimated for all of the samples (Fig. 4b).

The substitution of strontium for lanthanum resulted in the splitting of TPR curves as a consequence of an increase in the amount and variety of oxygen species (because of the formation of a more complicated microstructure). The reduction of trivalent cobalt also occurred in two steps. The first step $Co^{3+} \longrightarrow Co^{2+}$ occurred below 500°C with the retention of the perovskite structure (probably, because of the formation and ordering of anionic vacancies), whereas the second step was the bulk reduction $Co^{2+} \longrightarrow Co^0$ in the region of 500–900°C. However, doping with strontium facilitated the deep reduction processes $Co^{4+} \longrightarrow Co^0$ and $Co^{3+} \longrightarrow Co^0$. The former process, the reduction $Co^{4+} \longrightarrow Co^0$, occurred in the temperature region below 400°C; it is most likely that this process occurred in near-surface layers enriched in strontium (although the analogous process $Co^{4+} \longrightarrow Co^0$ also occurred in the temperature region of 400–500°C for a sample with

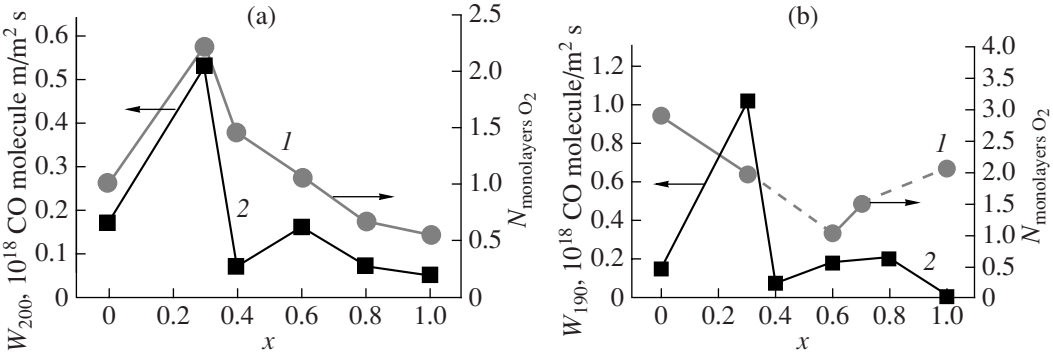

Fig. 4. Dependence of (*1*) the amount of consumed hydrogen in TPR temperature regions up to (a) 150 and (b) 130°C and (*2*) the rate of CO oxidation at (a) 200 and (b) 190°C on the composition (x) of samples from the series of $La_{1-x}Sr_xCoO_{3-y}$ calcined at (a) 900 and (b) 1100°C.

Table 5. Reduction of $La_{1-x}Sr_xCoO_{3-y}$ samples calcined at 900°C in separated regions of hydrogen uptake

x	Uptake regions (1 + 2) (40–500°C)	Uptake region (3) (500–900°C)	Cationic species ratio Co^{4+}/Co^{3+} (calculated from (1 + 2) and (3))
0	89% $Co^{3+} \longrightarrow Co^{2+}$ (380°C) 9% $Co^{3+} \longrightarrow Co^0$	89% $Co^{2+} \longrightarrow Co^0$ (650°C)	0.02/0.98
0.3	(1 + 2)*: 32% $Co^{4+} \longrightarrow Co^0$ (350°C): (3): 26% $Co^{3+} \longrightarrow Co^{2+}$ and 42% $Co^{3+} \longrightarrow Co^0$ (445°C)	(4 + 5): 26% $Co^{2+} \longrightarrow Co^0$ (635°C)	0.32/0.68
0.4	(1 + 2 + 3): 18% $Co^{4+} \longrightarrow Co^0$ and 28% $Co^{4+} \longrightarrow Co^{2+}$ (363°C) (4 + 5): 54% $Co^{3+} \longrightarrow Co^0$ (460°C)	(6 + 7): 28% $Co^{2+} \longrightarrow Co^0$ (603 C 760°C)	0.46/0.54
0.6	(1 + 2 + 3 + 4): 42% $Co^{4+} \longrightarrow Co^0$ (250, 300, 344, and 390°C) (5): 25% $Co^{3+} \longrightarrow Co^{2+}$ and 41% $Co^{3+} \longrightarrow Co^0$ (463°C)	(6 + 7 + 8): 25% $Co^{2+} \longrightarrow Co^0$ (614, 717 C 772°C)	0.42/0.66
0.8	(1): 13% $Co^{4+} \longrightarrow Co^0$ (283°C) (2): (475°C) 28% $Co^{3+} \longrightarrow Co^{2+}$ 51% $Co^{4+} \longrightarrow Co^0$ 9% $Co^{3+} \longrightarrow Co^0$	(3): 28% $Co^{2+} \longrightarrow Co^0$ (740°C)	0.66/0.3
1.0	(1 + 2 + 3): 91% $Co^{4+} \longrightarrow Co^0$ (up to 600°C)	7.4% $Co^{3+} \longrightarrow Co^0$ (600–900°C)	0.91/0.07

* In the case of peak splitting, the corresponding peak temperatures are specified for each particular peak or the greatest peak from the group of peaks due to the process.

$x = 0.7$). The latter, the reduction $Co^{3+} \longrightarrow Co^0$, can occur in the temperature region of 400–500°C ($x = 0.6$, 1.0) along with the process $Co^{3+} \longrightarrow Co^{2+}$ ($x = 0.6$).

In spite of the general tendency toward an increase in the reducibility of samples with increasing strontium fraction (x) with a shift of peak temperatures (T_{max}) to the region of lower TPR temperatures, the reduction of strontium cobaltite ($x = 1$) occurred continuously at higher temperatures ($T_{max} = 600$°C). It is likely that the shift of reduction peaks T_{max} to the region of higher temperatures was due to a decrease in the mobility of oxygen because of the formation of a vacancy-ordered phase of $SrCoO_{3-x}$.

$La_{1-x}Sr_xCoO_{3-y}$ samples at T_{calcin} = 900°C. The TPR curves of the samples calcined at 900°C were more split than those of the samples calcined at 1100°C. This can be explained by the even more complicated microstructure with the formation of the core–shell system, as evidenced by published data [4]. The complication of the microstructure not only increased the number of oxygen species but also changed the order of reduction processes: the removal of these species in the course of TPR occurred in somewhat another manner than that in the series of samples calcined at 1100°C.

Unsubstituted $LaCoO_3$ was also reduced in two steps: the cation reduction $Co^{3+} \longrightarrow Co^{2+}$ occurred in the region below 500°C, and the bulk reduction $Co^{2+} \longrightarrow Co^0$ occurred above 500°C. Analogously, an excessive consumption at low temperatures suggests the deeper reduction of a portion (9%) of Co^{3+} cations by the reaction $Co^{3+} \longrightarrow Co^0$ (Table 5). Figure 4a shows the estimated amount of weakly bound surface oxygen removed in the temperature region below 150°C (the numbers of removed monolayer surface coverages with oxygen were estimated for all of the samples).

In the entire series of substituted samples calcined at 900°C, doping with strontium facilitated the deep reduction processes $Co^{4+} \longrightarrow Co^0$ and $Co^{3+} \longrightarrow Co^0$. The former process, the reduction $Co^{4+} \longrightarrow Co^0$, occurred at temperatures below 400°C; it is most likely that this process also occurred in near-surface layers enriched in strontium (although the analogous process

$Co^{4+} \longrightarrow Co^0$ also occurred in the temperature region of 400–500°C in a sample with $x = 0.8$). The latter, the reduction $Co^{3+} \longrightarrow Co^0$, occurred in the temperature region of 400–500°C ($x = 0.6$, 1.0), and it occurred along with the process $Co^{3+} \longrightarrow Co^{2+}$ in samples with $x = 0.3$, 0.6, and 0.8.

Note that, according to the reaction scheme proposed, the reduction process $Co^{4+} \longrightarrow Co^{2+}$, which occurred in the temperature region below 400°C in a sample with $x = 0.4$, took place with the retention of the perovskite structure, probably by the formation of an anion-deficient phase of $La_{1-x}Sr_xCoO_{2.5}$. The reduction of this phase occurred above 500°C and corresponded to the bulk reduction process $Co^{2+} \longrightarrow Co^0$.

Unlike the sample from the previous series calcined at 1100°C, the reduction of strontium cobaltite occurred more discretely. This was likely due to the less perfect crystal structure; the following individual reduction processes can be recognized in it: $Co^{4+} \longrightarrow Co^0$ (to 600°C) and $Co^{3+} \longrightarrow Co^0$ (600–900°C).

Considering different orders (depending on the fraction of strontium) of reduction processes ($Co^{4+} \longrightarrow Co^{2+}$ and $Co^{4+} \longrightarrow Co^0$) for substituted cobaltites calcined at 900°C and the degrees of these processes (the reduction of Co^{4+} and Co^{3+} to Co^{2+} or deeper reduction to Co^0), we can assume the crucial effect of sample microstructures, as well as surface composition and structure. Thus, for example, for a sample with $x = 0.3$ ($T_{preparation} = 1100$°C), the deep reduction $Co^{4+} \longrightarrow Co^0$ can be explained, on the one hand, by the well-known enrichment of near-surface layers in highly charged Co^{4+} cations [4] and, on the other hand, by microstructure disordering because of a morphotropic transition, which facilitated the reduction and increased the degree of this process.

Thus, an analysis of the experimental data suggests the dependence of oxygen species and their reactivity characteristics on not only the sample composition (the strontium fraction x) but also synthesis conditions, which are responsible for the phase composition and microstructure of the sample. As demonstrated in this section, the role of this microstructure is a very important component responsible for the order of reduction processes.

Oxygen Species and Their Reactivity

In accordance with TPR data, we can assume the occurrence of the following oxygen species in the series of $La_{1-x}Sr_xCoO_{3-y}$ perovskites:

(1) weakly bound oxygen, which was removed in the course of TPR to 150°C;

(2) near-surface oxygen from the coordination environment of Co^{4+} cations, which was removed to 400°C by the reaction $Co^{4+} \longrightarrow Co^0$;

(3) lattice oxygen bound to Co^{4+} cations, which was removed in the region of 400–500°C by the reaction $Co^{4+} \longrightarrow Co^0$ ($x = 0.8$; $T_{calcin} = 900$°C and $x = 0.7$; $T_{calcin} = 900$°C);

(4) lattice oxygen bound to Co^{3+} cations, which was removed in the region of 400–500°C by the reactions $Co^{3+} \longrightarrow Co^{2+}$ and $Co^{3+} \longrightarrow Co^0$;

(5) lattice oxygen bound to Co^{2+} cations, which was removed above 500°C.

Considering particular oxygen species that are responsible for the activity of the LaSrCo series in deep oxidation reactions, let us compare hydrogen consumption data in different temperature regions with catalytic activity data.

(1) The low-temperature consumption (to 150°C) of hydrogen quantitatively corresponds to the removal of no more than one oxygen layer. Because phase reduction processes do not occur in this region, oxygen removed in the course of TPR belongs to the most weakly bound surface species (Tables 1, 2; Fig. 4). The calculated amount of hydrogen consumed in region (1) as a function of strontium concentration showed that this function has a maximum in the sample with $x = 0.3$ (Fig. 4, curve *1*), which correlates with changes in the specific catalytic activity in the reaction of CO oxidation (Fig. 4, curve *2*).

Thus, the specific catalytic activity of the series in the reaction of CO oxidation depends on the presence of weakly bound oxygen species, which can be adsorbed at the boundaries of microblocks, which were detected previously [4] using high-resolution electron microscopy.

The sample with $x = 1$ calcined at 1100°C is the exception. A possible explanation for this sample can be the fact that the available weakly bound oxygen species adsorbed at the anionic vacancies/interfaces of $SrCoO_{3-y}$, by analogy with the $SrFeO_{3-y}$ series (which was studied previously [7]), are easily removed by heating. Thus, oxygen species active in oxidation were absent from the given sample at the reaction temperature $T = 200$°C.

(2) The hydrogen uptake at temperatures up to ~500°C nonmonotonically changed with the concentration of strontium (Tables 1, 2; Fig. 2). In this case, an increase in the concentration of strontium led to a decrease in reduction temperatures, except for samples with $x = 1$ calcined at 900 and 1100°C. The hydrogen uptake in this region corresponds to the removal of one to ten oxygen monolayers. The calculated data on the hydrogen uptake in this temperature region indicate that, most likely, oxygen was removed in this case from the coordination sphere of Co^{3+} cations and highly charged Co^{4+} cations. Tables 4 and 5 summarize the amounts of Co^{3+} and Co^{4+} cations calculated from the hydrogen uptake in regions (2) and (3). These calculations demonstrated the absence of correlations between changes in the specific catalytic activity in CO oxidation and the hydrogen uptake in this temperature region and between the amount of Co^{4+} in a sample with com-

position x and the character of changes in the specific catalytic activity in the series of $La_{1-x}Sr_xCoO_{3-y}$.

(3) The hydrogen uptake in the temperature region above 500–900°C quantitatively corresponded to the deep reduction processes $Co^{2+} \longrightarrow Co^0$ accompanied by the degradation of the perovskite structure. Stepwise reduction in the region of high TPR temperatures, which was particularly pronounced in samples with x = 0.3 and 0.6 calcined at 1100°C, can be due to structural rearrangements: the ordering of anionic vacancies formed in the course of oxide reduction and accompanied by the formation of vacancy-ordered phases of $(LaSrCo)O_{3-\alpha}$ with different values of α, as proposed by Royer et al. [6]. The total amount of hydrogen consumed from the onset of the experiment to the temperature region of 900°C did not correlate with changes in the specific catalytic activity in CO oxidation.

Thus, the experimental data allowed us to hypothesize that strongly bound lattice oxygen species in perovskites from the series of $La_{1-x}Sr_xCoO_{3-y}$, including those from the coordination environment of highly charged cations, do not participate in the oxidation of CO. A correlation between the amount of weakly bound oxygen and the activity of samples in the process of CO oxidation may be indicative of the leading role of weakly bound surface species in the formation of catalytic properties of the series in deep oxidation reactions. In this case, weakly bound oxygen can be inserted into the walls of microblocks/microdomains, which were detected previously for x = 0.3 using high-resolution electron microscopy [4].

Phase Formulas: Oxygen Nonstoichiometry and the Number of Co^{4+}/Co^{3+} Cations

As noted above, Table 3 summarizes the oxygen nonstoichiometry y for each particular sample from the series of $La_{1-x}Sr_xCoO_{3-y}$ and the ratios between Co^{4+} and Co^{3+} cations calculated from the total uptake. In addition, the amounts of Co^{3+} and Co^{4+} cations were calculated from the hydrogen uptake in regions (2) and (3) (Tables 4, 5). Note a good agreement between the ratios of Co^{4+} and Co^{3+} cations calculated from the total uptake (Table 3) and from individual peaks (Tables 4, 5). As a rule, the calculated concentrations coincided (10%); that is, they were within the limits of the accuracy of TPR. As a rule, the observed discrepancies, which did not fall outside the limits of this accuracy, were associated with an excess of oxygen, which can be embedded in interblock boundaries [4]. Thus, we obtained a good correlation between the calculated amounts of Co^{4+} cations, the oxygen nonstoichiometry y (Fig. 3), and the published values. Petrov et al. [5] hypothesized that, in samples prepared by ceramic processing with $x < 0.4$, charge compensation upon strontium substitution occurred by an increase in the charge on cobalt cations (Co^{4+}) and a maximum concentration of Co^{4+} was reached at $x = 0.4$. For samples with $x > 0.4$, charge compensation occurred by the formation of oxygen vacancies. The fraction of vacancies also increased with temperature.

Effect of the Preparation Procedure on the Oxygen Species and Their Reactivity

Let us characterize the effect of preparation procedure on oxygen species and their reactivity for the series of $La_{1-x}Sr_xCoO_{3-y}$ and on the oxygen nonstoichiometry and the distribution of Co^{4+}/Co^{3+} cations.

From data in Tables 1 and 2, it follows that the consumption (TPR peak intensity) decreased with calcination temperature in temperature regions (1) and (2), and the reducibility of the system decreased. An increase in the consumption in temperature region (3) with increasing synthesis temperature implies a redistribution of oxygen species and their concentrations; correspondingly, the fraction of highly charged Co^{4+} cations decreased. As the calcination temperature was increased, the reduction peaks shifted to the region of higher temperatures. In this case, the observed changes were not directly related to a decrease in the specific surface area of samples. However, they may be related to changes in the surface structure/composition as the calcination temperature was increased. Thus, the surface enrichment in strontium and cobalt (Co^{4+}) is well known from SIMS data [4].

An increase in the calcination temperature leads to a decrease in the concentration of Co^{4+} cations and, correspondingly, a decrease in the hydrogen uptake in corresponding temperature regions (2), that is, to 500°C. In this case, the character of changes in the concentration of Co^{4+} as a function of x, which changed symbatically with nonmonotonic changes in the hydrogen uptake in temperature region (2) (Fig. 2, curves *1*), exhibited a maximum in samples with x = 0.4 and 1. In Table 4, it can be seen that the concentrations of Co^{4+} cations were 64 and 80% for samples with x = 0.8 and 1.0, respectively, calcined at 900°C. Petrov et al. [5] found that the maximum concentration of Co^{4+} cations was ~32% for a sample of $La_{0.6}Sr_{0.4}CoO_{3-y}$ ($x = 0.4$) prepared by traditional ceramic processing. The observed peculiarities were due to the microstructure and composition of surface/near-surface layers of mechanochemically prepared samples characterized by the segregation of strontium and cobalt in the near-surface layer [4], as compared with the ceramic series [5].

Thus, an increase in the calcination temperature caused a decrease in the amounts of oxygen removed in low-temperature and medium-temperature regions (1) and (2), respectively. The corresponding TPR peaks shifted to the region of higher temperatures; that is, the reducibility of the series decreased. It is likely that the observed reduction behavior was due to the specific features of mechanochemical synthesis.

In general, note the difference of the reduction of substituted cobaltites from the series of $La_{1-x}Sr_xCoO_{3-y}$ from the results of analogous TPR studies of

$La_{1-x}Ca_xFeO_{3-y}$ and $La_{1-x}Sr_xFeO_{3-y}$ ferrite and $La_{1-x}Ca_xMnO_{3+d}$ manganite systems, which were described in detail elsewhere [9–11]. It is well known that the reactivity (in this case, reducibility) of cobaltites is higher than that of manganites or, especially, ferrites [1]. Thus, the bulk reduction of lanthanum ferrite came into play as the temperature was increased to 900°C, whereas this reduction of lanthanum cobaltite was complete even at 700°C. Moreover, LaSrCo perovskites are characterized by stepwise reduction, which occurs through the formation of anion-deficient phases (by analogy with published data [6]), as can be clearly seen from the shapes of TPR curves in the regions of low and high experiment temperatures. A special feature of the reduction of $La_{1-x}Sr_xCoO_{3-y}$ cobaltites is the occurrence of the bulk reduction $Co^{2+} \longrightarrow Co^0$ in the region of high temperatures (500–700°C). However, the bulk reduction of ferrites or manganites implies the process $Fe^{3+} \longrightarrow Fe^0$ (above 600–800°C depending on the dopant content x) or $Mn^{3+} \longrightarrow Mn^{2+}$ (above 600°C), respectively. Thus, unlike ferrites and manganites, the bivalent transition metal cation (Co^{2+}) in cobaltites is stable in the perovskite structure, probably because of the formation of a vacancy-ordered phase of $La_{1-x}Sr_xCoO_{2.5}$.

CONCLUSIONS

(1) In this work, oxygen species in the series of $La_{1-x}Sr_xCoO_{3-y}$ and the reactivity of these species were studied using TPR. The reduction of $La_{1-x}Sr_xCoO_{3-y}$ perovskites occurred in three temperature regions.

(2) In the TPR temperature region below 400°C, the near-surface processes $Co^{4+} \longrightarrow Co^0$ occurred. In the TPR temperature region of 400–500°C, the bulk reduction $Co^{3+} \longrightarrow Co^0$, which nonmonotonically increased with the fraction of strontium, occurred along with the reduction $Co^{3+} \longrightarrow Co^{2+}$, which occurred with the retention of the perovskite structure. At high temperatures (above 500°C), the bulk reduction $Co^{2+} \longrightarrow Co^0$ always occurred. The particular reaction scheme depended on sample composition and preparation conditions, which are responsible for the sample microstructure. The TPR of mechanically activated samples from the series of $La_{1-x}Sr_xCoO_{3-y}$ was accompanied by structure rearrangements with the formation of vacancy-ordered phases of $(LaSrCo)O_{3-y}$ with different values of y (as hypothesized previously [6]).

(3) An increase in the strontium content of the samples increased the amount and reactivity of oxygen species.

(4) The overall reducibility of the samples decreased with calcination temperature. It was found that the observed differences were related to the microstructure peculiarities and composition of surface/near-surface layers of mechanochemically prepared samples, which are characterized by the segregation of strontium and cobalt in a near-surface layer.

(5) Based on the results of TPR, the occurrence of the following oxygen species can be assumed:

• weakly bound oxygen, which is released in the course of TPR below 150°C;

• surface/near-surface oxygen from the coordination environment of Co^{4+} cations, which is released up to 400°C;

• lattice oxygen bound to Co^{4+} cations, which is released up to 500°C;

• lattice oxygen bound to Co^{3+} cations, which is released up to 500°C;

• lattice oxygen bound to Co^{2+} cations, which is released above 500°C.

(6) A correlation between the amount of weakly bound oxygen and the activity of samples in the oxidation of CO was found. This may be indicative of the leading role of weakly bound surface species in the formation of the catalytic properties of the test sample series in deep oxidation reactions. In this case, weakly bound oxygen can be inserted into the walls of microblocks/microdomains. No correlation between the amount of strongly bound (lattice) oxygen removed upon TPR and the activity of $La_{1-x}Sr_xCoO_{3-y}$ samples in the oxidation of CO was found.

REFERENCES

1. Tejuca, L.G., Fierro, J.L.G., and Tascon, J.M.D., *Adv. Catal.*, 1989, vol. 36, p. 237.
2. Baran, E.J., *Catal. Today*, 1990, vol. 8, no. 2, p. 133.
3. Yamazoe, N. and Teraoka, V., *Catal. Today*, 1990, vol. 8, no. 2, p. 175.
4. Isupova, L.A., Alikina, G.M., Tsybulya, S.V., Boldyreva, N.N., Kryukova, G.N., Yakovleva, I.S., and Sadykov, V.A., *Int. J. Inorg. Mater.*, 2001, vol. 3, p. 559.
5. Petrov, A.N., Kononchuk, O.F., Andreev, A.V., Cherepanov, V.A., and Kofstad, P., *Solid State Ionics*, 1995, vol. 80, p. 189.
6. Royer, S., Alamdari, H., Duprez, D., and Kalyaguine, S., *Appl. Catal., B*, 2005, vol. 58, p. 273.
7. Isupova, L.A., Yakovleva, I.S., Alikina, G.M., Rogov, V.A., and Sadykov, V.A., *Kinet. Katal.*, 2005, vol. 46, no. 5, p. 773 [*Kinet. Catal.* (Engl. Transl.), vol. 46, no. 5, p. 729].
8. Futai, M. and Yonghua, Ch., *React. Kinet. Catal. Lett.*, 1986, vol. 31, no. 1, p. 47.
9. Isupova, L.A., Yakovleva, I.S., Alikina, G.M., Rogov, V.A., and Sadykov, V.A., *Kinet. Katal.*, 2005, vol. 46, no. 5, p. 773 [*Kinet. Catal.* (Engl. Transl.), vol. 46, no. 5, p. 729].
10. Yakovleva, I.S., Isupova, L.A., Rogov, V.A., and Sadykov, V.A., *Kinet. Katal.*, 2008, vol. 49, no. 2, p. 274 [*Kinet. Catal.* (Engl. Transl.), vol. 49, no. 2, p. 261].
11. Isupova, L.A., Yakovleva, I.S., Rogov, V.A., Alikina, G.M., and Sadykov, V.A., *Kinet. Katal.*, 2004, vol. 45, no. 3, p. 473 [*Kinet. Catal.* (Engl. Transl.), vol. 45, no. 3, p. 446].